Deregulation in binding and expression of RNA binding proteins as a mechanism of CD19-negative B-ALL

Nicole Ziegler
University Medical Center of the Johannes Gutenberg University Mainz
Mariela Cortés-López
Institute of Molecular Biology https://orcid.org/0000-0002-8951-4811
Francesca Alt
University Medical Center of the Johannes Gutenberg University Mainz
Maximilian Sprang
Johannes Gutenberg University Mainz
Nadine Lehmann
University Medical Center of the Johannes Gutenberg University Mainz
Khalifa El Malki
University Medical Center of the Johannes Gutenberg University Mainz
Arthur Wingerter
University Medical Center of the Johannes Gutenberg University Mainz
Alexandra Russo
University Medical Center of the Johannes Gutenberg University Mainz
Olaf Beck
University Medical Center of the Johannes Gutenberg University Mainz
Sebastian Attig
University Medical Center of the Johannes Gutenberg University Mainz
Lea Roth
University Medical Center of the Johannes Gutenberg University Mainz
Julian König
Institute of Molecular Biology
Claudia Paret (claudia.paret@unimedizin-mainz.de)
University Medical Center of the Johannes Gutenberg University Mainz
Jörg Faber
University Medical Center of the Johannes Gutenberg University Mainz

Article

Keywords:

Posted Date: May 23rd, 2022

DOI: https://doi.org/10.21203/rs.3.rs-1630084/v1

Abstract

Despite massive improvements in the treatment of B-ALL through CART-19 immunotherapy, a large number of patients suffer a relapse due to loss of the targeted epitope. Mutations in the *CD19* locus and aberrant splicing events are known to account for the absence of surface antigen. However, the molecular determinants are not fully enlightened so far. We applied deep sequencing to analyze the *CD19* locus in a cohort of B-ALL patients and identified a blast-specific 2-nucleotide deletion in intron 2 that exists in 35% of samples at initial diagnosis. Remarkably, no disease-specific mutation in the coding region was detected. We show that this deletion affects the binding site of RNA binding proteins (RBPs) including PTBP1. Moreover, we show that downregulation of PTBP1 in 697 cells reduces CD19 total protein by increasing intron 2 retention. Isoform analysis in patient samples revealed that blasts, at diagnosis, express increased amounts of CD19 intron 2 retention compared to normal B cells. By RNAseq and qRT-PCR, we could identify several RBPs being deregulated in leukemic blasts.

Our data suggest that loss of RBP functionality by mutations altering their binding motifs or by deregulated expression might harbor the potential for the disease-associated accumulation of therapy-resistant CD19 isoforms.

Introduction

Despite tremendous improvements in the treatment of B-ALL during the last years, the prognosis for those patients suffering a relapse is rather poor. Immunotherapy with chimeric antigen receptor (CAR)-T cells targeting CD19 appeared to be a game changer, leading to impressive remission rates in pediatric patients with relapsed or refractory ALL (1, 2). However, up to 50% of B-ALL patients receiving CAR-T cells develop disease relapse, 30–60% of them being characterized by target antigen loss (3–7). Recent research already identified genetic alterations in the CD19 locus that are attributed to epitope-negative protein variants (8). Furthermore, a number of alternative splicing events such as exon 2 skipping, deletion of exons 5–6 and intron 2 retention could be related to CD19-negative relapse (9–12). Some of those isoforms already exist at diagnosis (13). The consequences of mis-splicing are thereby diverse and, moreover, might overlap with genetic variations.

Splicing events are mediated by RNA binding proteins (RBPs) that coordinate the incorporation of exons into the mature mRNA. In respect to CD19, mechanistic studies could already associate one factor, namely SRSF3, to alternative splicing events leading to antigen loss (9).

Along this line, we analyzed the sequence of the CD19 locus and the expression profile of RBPs in blasts at diagnosis compared to normal B cells. Our data suggest that disease-associated genetic mutations in RBP binding motifs as well as the deregulation of splicing modulators may lay the foundation for the prevalence of therapy-resistant CD19 isoforms by intervening in the functional network of RBPs.

Material And Methods

Sample Cohort

All pediatric B-ALL patients were treated according to the COALL 08–09 study protocol (v. 01.10.2010). The total number of B-ALL patients analyzed was 36, 69% of them being diagnosed with common-ALL and 28% with pre-B-ALL, one patient with pro-B-ALL (Table S1). Patients of the control group were hospitalized due to a non-hematologic malignancy. Bone marrow or peripheral blood was obtained as surplus material during standard diagnostic procedures. Subsequent analysis was performed with the consent of the patients or patient's parents in agreement with the ethics committee of Rhineland-Palatinate (no. 2018–13713). Samples were handled in accordance with the Declaration of Helsinki. Remission was defined as < 5% blast cells.

DNA sequencing

Exon 1 to 4 including introns of the CD19 locus (chr16:28942047–28944969) was amplified with the Expand long template Polymerase system (Roche, Basel, Switzerland). Paired-end libraries were created following the Nextera XT protocol (Illumina, San Diego, CA, USA) and subjected to deep sequencing on an Illumina MiSeq sequencer according to standard procedures. Minimum depth of coverage was 1000x. Data were processed using BWA Enrichment v1.0 for the generation of BAM files and the somatic variant caller of Illumina, which allows to detect low-frequency mutations (below 5%). Analysis of variants was performed with the VariantStudio software (Illumina). Variants with a population frequency less than 5% were further analyzed. Reads were visualized using the IGV software.

Prediction of RBP binding sites

RBP binding motifs were predicted using the website service of the AtTRACT database (14). As input, we used the sequence of the *CD19* locus (exons 1 to 3) and selected motifs of at least 4 nucleotides in length. We collapsed overlapping motifs per RBP using custom R scripts based in the GenomicRanges package.

RNA-Seq

RNA was extracted with the miRNeasy kit (QIAGEN, Hilden, Germany). Only samples with a RIN > 8 were used for library preparations using the Illumina® TruSeq® Targeted RNA Expression kits to perform multiplexed gene expression profiling. Libraries were subjected to sequencing on an Illumina MiSeq sequencer according to standard protocols. Data was processed in the Illumina® BaseSpace Sequence Hub to extract the raw counts. Counts were analyzed with DESeq2 to determine differentially expressed genes. Two *HPRT1* targets were used as controls to estimate the size factors before differential analysis and normalization. Log-transformed raw counts were used for heatmap visualization.

Flow cytometric immunophenotyping

Immunophenotyping was performed with bone marrow aspirates or peripheral blood following standard diagnostic procedures as described previously (13). Samples containing > 80% leukemic blasts were chosen for cell sorting.

Isolation of PBMCs

For isolation of peripheral blood mononuclear cells (PBMCs), bone marrow was diluted with PBS + 2mM EDTA and separated by density gradient centrifugation (800xg, 30min) using Histopaque®-1077 (Merck KGaA, Darmstadt, Germany). PBMCs were washed and immediately frozen in FCS + 10% DMSO.

Fluorescence-activated Cell Sorting (FACS)

Cells isolated from bone marrow were stained at room temperature for 15min in the dark. 7-aminoactinomycon D (7-AAD) and anti-CD45 antibody were used for cells from leukemia patients, 7-AAD and anti-CD19 (all Beckman Coulter, Pasadena, CA, USA) for cells from healthy donors. Sorting was performed in MACS buffer (PBS, 2mM EDTA, 0.1% BSA) using a FACS Aria (Becton Dickinson, Franklin Lakes, NJ, USA). Normal B cells and leukemic blasts were defined as 7-ADD$^-$/CD19$^+$ and 7-ADD$^-$/CD45^{low}, respectively.

RNA extraction and cDNA synthesis

Total RNA from sorted cells was purified using the ReliaPrep™ RNA Cell Miniprep System (Promega, Madison, WI, USA) following the manufacturer's protocol. Reverse transcription was performed with the PrimeScript™ RT Reagent Kit with gDNA Eraser (TaKaRa, Kusatsu, Japan).

Quantitative RT-PCR (qRT-PCR)

qRT-PCR was performed using the PerfeCTa® SYBR® Green Fast Mix® (Quantabio, Beverly, MA, USA) in a LightCycler 480 instrument (Roche). For sequences of primers for RBPs and CD19 isoforms see Table S7. Raw values were normalized to *HPRT*.

Semi-quantitative RT-PCR

Semi-quantitative RT-PCR was performed using cDNA of FACS-sorted B cells and leukemic blasts. To amplify CD19 isoforms, primers spanning exon 1 to exon 4 (Table S7) and Taq-DNA polymerase I (Axon Labortechnik, Kaiserslautern, Germany) were used. PCR conditions were as follows: 94°C 5min, 35 cycles of 94°C 30s, 60°C 30s, 72°C 1min, 72°C 10min. Fragments were visualized using a QIAxcel® DNA High Resolution Cartridge on a QIAxcel Advanced instrument (QIAGEN) running the standard protocol.

Knockdown experiments in 697 cells

For CRISPR/Cas9 experiments in 697 cells, 2 gRNAs for each target were used, applying a Dual-Guide approach. crRNA:tracrRNA duplex formation and RNP assembly were performed for each gRNA separately following a protocol for electroporation of human B cell lines provided by the manufacturer (IDT, Coralville, IA, USA). For transfection, 1x10^6 cells were resuspended in Electroporation Buffer (Bio-Rad, Hercules, CA, USA) and electroporated using a GenePulser Xcell device (Bio-Rad) with the following settings: square wave, 1 pulse, 250V, 2ms. Predesigned crRNAs for *PTBP1* and *PTBP2* (Hs.Cas9.PTBP1.1.AA, Hs.Cas9.PTBP1.1.AB, Hs.Cas9.PTBP2.1.AB, Hs.Cas9.PTBP2.1.AD) and accessory reagents were from IDT. Cells were collected 72h after nucleofection.

Western Blotting

Cell pellets were lysed in RIPA buffer containing protease inhibitor cocktail (Roche). SDS-Page and Western blotting was performed following standard procedures. Primary antibodies were as follows: PTBP1 (Cell Signaling, Danvers, MA, USA), PTBP2 (abcam, Cambridge, UK), CD19 (Cell Signaling), Histon H3 (Cell Signaling), GAPDH (Cell Signaling). Signal detection and quantification was performed using a Fusion Pulse imaging system (Vilber, Eberhardzell, Germany).

Statistical analysis

Data is shown as mean ± SD. Statistical significance was analyzed by two-tailed Student's *t* test (GraphPad Prism software version 9.0.1). *p* values < 0.05 were considered significant.

Results

B-ALL patients feature disease-specific mutations in the CD19 locus at initial diagnosis

The cellular mechanisms that potentially account for epitope loss are diverse, mutations in the gene encoding for the targeted antigen itself being one of them. As most CART-19 therapy-resistant protein variants identified so far result from exon 2 deletions or inaccurate excision of adjacent introns, we performed mutation analysis of the genomic sequence comprising exon 1 to 4 including introns. We analyzed 3 controls and 20 pediatric B-ALL patients at initial diagnosis and, out of those, 15 samples in remission by deep sequencing (Table S1). Strikingly, we identified a small deletion (NM_001178098.1:c.356 − 95_356-94delCT, derived from TTC > TTC/T at position 28944127) with an allele frequency of ~ 1% located in intron 2 (Tables S2, S3, Fig. 1A) in 35% of samples at diagnosis, both in common and pre-B-ALL, but not in the control group. Remission samples of the same patients did not harbor this genetic variant, indicating its specificity to leukemic blasts. In one sample from initial diagnosis another intronic mutation (NM_001178098.1:c.356-111A > G) was detected. It was located next to the NM_001178098.1:c.356 − 95 locus and featured an allele frequency of 50% in our sample while showing a particularly low allele frequency (0.12%) in the cohort of the 1000 Genomes Project (https://www.internationalgenome.org). However, as material of the same patient in remission was not available, we cannot judge whether the mutation is associated to leukemic blasts. Interestingly, our analysis did not reveal any blast-specific mutation affecting the coding region of CD19.

Thus, our results indicate that subclonal, intronic mutations already exist in leukemic blasts at diagnosis.

Disease-specific Mutations In Cd19 Affect Rbp Binding Sites

We next investigated whether the small deletion in CD19 intron 2 might overlap with recognition motifs for splicing factors and thereby alter the landscape of cis-regulatory elements. The ATtRACT database predicted PTBP1 and ZFP36 to bind to this locus (Fig. 1B). Although we found a high frequency of PTBP1 binding sites throughout the analyzed sequence, the abundance of long and thereby more specific motifs accumulate in intron regions and, remarkably, most prominently in intron 2 (Fig. S1, 1B). We assume an outstanding function of this dedicated locus, as the optimal binding site for PTBP1 is the core sequence TCTTCT embedded in a longer pyrimidine tract (15, 16). Exactly the same motif is affected by the NM_001178098.1:c.356 – 95_356-94delCT deletion, furthermore shortening the pyrimidine tract downstream of the consensus sequence. Thus, we conclude that this blast-specific mutation has a considerable impact on PTBP1 binding.

In order to determine the role of PTBP1 and ZFP36 in B cell leukemia and to figure out whether their expression might be associated with the disease state, qRT-PCR analysis was performed in sorted blasts and B cells (Fig. 1C). Although not reaching significance due to high patient-to-patient variability, *PTBP1* showed lower mRNA abundance in blasts of 77% of patients compared to the average expression in B cells. Other than *PTBP1*, transcription of *ZFP36* was rather low in all our samples. Yet, it was significantly less expressed in blasts than in B cells.

Expression Of Rbps Is Deregulated In B-all Patients

Single splicing factors have already been associated with CD19 exon 2 processing. In order to investigate other relevant RBPs that might impact CD19 protein processing, we extended the search for RBP binding sites to the genomic region spanning exon 1 to exon 3. We thereby considered only those motifs ranging between 4 and 10 nucleotides, resulting in a list of 54 RBPs (Fig. S1). Expression levels of the same splicing factors were analyzed by targeted RNA-Seq in 9 patient samples of initial B-ALL diagnosis, 16 in remission and of 2 healthy donors to investigate a disease-associated expression profile (Fig. 2A). Pairwise comparisons revealed 20 differentially expressed genes (DEGs) in blasts relative to B cells, while 10 and 40 DEGs were found comparing remission samples to blasts or B cells, respectively (Tables S4-S6). Overall, the majority of RBPs were highest expressed in B cells, which is most likely also a result of cell sorting of these specimens. Going along with a comparatively small amount of B cells in the remission samples indicated by low levels of CD19, expression relative to blasts and B cells was mostly decreased.

The z-score revealed that *PTBP1* and *ZFP36* were higher expressed in B cells than in leukemic blasts, corroborating our qRT-PCR data (Fig. 2B, Table S4). To validate the disease-associated expression pattern of selected RBPs, the RNA-Seq data was corroborated by qRT-PCR analysis of leukemic blasts of pediatric B-ALL patients and normal B cells (Fig. 2C, D). Isolation by FACS thereby allowed cell type-related conclusions (Fig. S2). Consistently, *PTBP2*, a well-described paralog of PTBP1, was in tendency less expressed in isolated leukemic blasts than in B cells. *TIA1* did not significantly differ between both cohorts. While *SRSF1* expression was unchanged, *SRSF3* significantly decreased in blasts compared to B

cells. This, however, was not confirmed by targeted RNA-Seq, where it did not appear as DEG. In contrast, RNA-Seq suggested *SRSF7* as well as RBM5 to be decreased in blasts relative to B cells, which could not be confirmed in the sorted cells. Interestingly, *NONO*, which is associated with tumorigenesis in many types of cancer, was significantly less expressed in blasts than in B cells. RNA-Seq also implied differential expression of *YTHDC1* and *PABPN1*. This, however, could not be corroborated by qRT-PCR analysis. Despite discrepancies between both types of analysis for some of the RBPs, explainable by variations in sample preparation, different patient cohorts used for the two types of experiments and a high patient-to-patient variability, our data reveal a disease- and patient-specific expression pattern of several RBPs that implies a correlation with the occurrence of particular CD19 isoforms.

Thus, beyond the appearance of intron-specific mutations that may affect the binding of certain RBPs, we show that the expression of such RBPS is generally deregulated in B-ALL.

Ptbp1 Is A Regulator Of Cd19 Intron 2 Splicing

Focusing on PTBP1, we observed a positive correlation between *PTBP1* and *CD19* mRNA expression in blasts at diagnosis (Fig. 3A). In order to investigate whether this effect might result from alternative CD19 splicing mediated by PTBP1, we performed CRISPR/Cas9-mediated knockdown in the leukemic cell line 697 (Fig. 3B). As PTBP2 has similar function as PTBP1 and both factors can compensate for each other, we also performed a knockdown of *PTBP2* (Fig. S3A). qRT-PCR revealed that downregulation of *PTBP1* induced an increase in *PTBP2* expression, confirming the functional relevance of the reduction of *PTBP1* levels (Fig. 3C). It is known that PTBP1 regulates PTBP2 levels by alternative splicing mediating nonsense-mediated decay, which potentially holds true also in our cellular model (17). Consistent with the positive correlation seen in our patient cohort, levels of CD19 total protein were approximately halved upon *PTBP1* knockdown while a decrease in *PTBP2* expression did not significantly change *CD19* expression (Fig. 3D). Moreover, levels of CD19 surface expression were markedly reduced after *PTBP1* knockdown (Fig. S3B). Decreased CD19 protein abundance due to *PTBP1* KD was accompanied by an altered isoform composition (Fig. 3E). While the exon 2 WT variant as well as isoforms harboring exon 2 complete or partial deletion were less abundant, intron 2 retention (In2Ret) was significantly upregulated (Fig. 3F). Knockdown of *PTBP2*, however, did not affect isoform distribution. These data clearly suggest that deregulation of PTBP1, caused either by expression changes or alteration in binding capabilities, imply an accumulation of epitope-negative splicing variants that finally result in decreased levels of CD19 protein.

Intron 2 Retention Is Increased In Blasts Compared To Normal B Cells

In order to investigate whether leukemic blasts from patients at diagnosis and normal B cells generally differ in the expression of CD19 isoforms, we analyzed the occurrence of CD19 variants focusing on exon

2 processing. Consistent with previous results, in leukemic blasts both exon2-deleted CD19 variants (*ΔEx2* and *ΔEx2part*), were already present at diagnosis (Fig. 4A). Additionally, we detected intron 2 retention, which has so far been analyzed only in pre- and post-CART-19 samples. All three mis-spliced CD19 isoforms were expressed also in B cells (Fig. 4B), suggesting that aberrant splicing does equally occur in healthy people. Consequently, the mere presence of the *CD19* variants analyzed here is not per se predictive for the disease. However, the accumulation of dedicated isoforms might make a big difference by shifting their ratio and disbalance their regular equilibrium. To investigate this issue in our patient cohort, we precisely quantified the expression of *CD19* variants by qRT-PCR using isoform-specific primers (Fig. 4C, Table S7). The high patient-to-patient variability observed before was equally visible in the present analysis, wherefore we did not detect significant differences in isoform expression between blasts and B cells. However, the majority of blast samples showed lower levels of *Ex2 WT* compared to B cells. Abundance of *ΔEx2* and *ΔEx2part* did not show apparent differences between groups and *ΔEx5-6* was hardly expressed in all of our samples. Levels of total *CD19* were, similar to the *Ex2 WT* variant, extremely different across sample groups. For better interpretation of isoform distribution, we calculated the percentage of each exon 2-related variant showing that leukemic blasts had elevated levels of *In2Ret* compared to B cells (Fig. 4D). At the same time, the regularly spliced WT isoform was in tendency less expressed, suggesting that the shift toward the mis-spliced variant happens at the expense of the regular one. Further analysis corroborated this finding, revealing negative correlation of the percentage of the exon 2 WT isoform related to intron 2 retention (Fig. 4E). Although the increase in *In2Ret* could not be decidedly attributed to the expression levels of *PTBP1* in the patient samples (Fig. 4F), we assume a prominent role of PTBP1 for CD19 exon 2 splicing. The effects of single RBPs might at least partially be masked by the general deregulation of the CD19 splicing machinery that we observe in the patient cohort. We show that the abnormal RBP expression profile in leukemic blasts already establishes at onset of the disease.

Discussion

The approval of CD19-directed immunotherapies dramatically improved the prognosis of patients with relapsed or refractory B-ALL and B cell lymphomas. However, about 30–50% of patients suffer a relapse, up to 60% of them being CD19-negative (1, 3, 6).

Besides genetic mutations, splicing variation of CD19 can lead to epitope loss and the escape from CAR-T cell-mediated elimination. While some publications assume a direct correlation between alternative splicing events and the emergence of immunotherapy-resistant CD19 isoforms, others suggests that genetic mutations in the CD19 locus are responsible for epitope-negative relapse (8, 9, 11). In some cases, however, the allele frequency of dedicated mutations was rather low, precluding CD19-specific genetic alterations as the mere mechanism of immune evasion (10). Thus, both CD19-specific frameshift mutations and splicing aberrations might coexist and jointly contribute to a disease-relevant expression pattern of CD19 variants. Whether these events occur already at diagnosis or establish under the pressure of conventional or CAR-T cell therapy is not known so far.

We show that mutations in intron sequences affect CD19 splicing by changing the binding site for RBPs. Strikingly, such mutations were detected already at diagnosis. This suggests that leukemic blasts harbor the potential to evolve into CAR-T-resistant clones directly from the beginning, exceeding the idea of Rabilloud et al. who claimed the existence of CD19-negative B-ALL cells prior CAR-T treatment (12).

Given the low allele frequency of the mutation, it is obviously subclonal and its relevance for the etiology of B-ALL remains to be elucidated. Whether it might be selected during disease progression or under therapy pressure could not be clarified so far as no samples at relapse under CART-19 therapy were available for this analysis.

Particularly, the blast-specific mutation identified in this work was predicted to affect the consensus motif of PTBP1. As splicing regulation by PTBPs mostly rely on the presence of several binding sites lying in close proximity (17), their high abundance rather support than mitigate the relevance of this dedicated binding motif. Our in vitro studies revealed that PBP1 mediates alternative splicing of exon 2, thereby regulating CD19 protein abundance. This mechanism aligns with our patient data showing positive correlation between *PTBP1* and *CD19* mRNA expression in blasts. Moreover, decreased *PTBP1* abundance in patients at diagnosis compared to controls appeared to go along with an increase in intron 2 retention.

Similar mechanisms are already known as somatic mutations that disturb regulatory sequences or alter the expression of RBPs are a common cause of cancer-specific alternative splicing (18–21). Functionally, isoform switches can influence protein stability, interactions and metabolic processes that finally translate into a selective advantage for tumor cells (22, 23). Interestingly, we did not find any blast-specific mutations in the coding sequence. Thus, frameshift mutations may occur later during disease development or rather under therapy and a potential correlation with the treatment regimen before CART-19 therapy should be considered.

The blast-specific indel might also affect the binding of ZFP36. ZFP proteins regulate cell quiescence and proliferation of B cells and promote VDJ recombination, consequently influencing B cell development and identity (24–26). However, it could not be associated with CD19 expression or splicing so far. We show that *ZFP36* is significantly less expressed in blasts than in B cells, corroborating its potential impact on disease-specific splicing aberrations. Both PTBP1 and ZFP36 are present throughout B cell development whereby PTBP1 and CD19 underlie expression changes depending on the developmental level (27–29). Consequently, the effects of single RBPs and protein-protein interactions on CD19 splicing might be influenced by the B cell stage or rather the leukemia phenotype. Unfortunately, due to the small patient cohort being available for cell sorting, we could not investigate this issue with an adequate number of samples in the present study.

We expanded the expression analysis of RBPs in blasts of pediatric leukemia patients at initial diagnose and in normal B cells by further splicing factors that were selected based on our screening data and literature search (9, 29–31). SRSF3 is required for exon 2 inclusion as evidenced by patient data revealing that its expression is decreased in relapsed leukemia while the *CD19 Δex2* isoform is increased (9). We

show that *SRSF3* transcription is already reduced in blasts at initial diagnosis. This, however, does not correlate with an increased abundance of *CD19 Δex2* in our sample cohort. Consistent with our hypothesis of a dominant CD19 isoform establishing during disease progression, we assume that the impact of SRSF3 deficiency on CD19 isoform selection might differ between the onset and later stages of the disease or even at relapse. Thus, we do not necessarily anticipate an accumulation of epitope-negative isoforms to be visible already at diagnosis.

Besides *SRSF3* and *ZFP36*, *NONO* was significantly less expressed in blasts compared to B cells. It could not be associated with leukemia progression or CD19 splicing so far, so that further investigations will be needed to evaluate its potential impact on disease-associated splicing events in B-ALL.

High patient-to-patient variabilities clearly exacerbate the evaluation of relevant correlations and coherencies. Nevertheless, similar expression of RBPs in B cells and blasts do not preclude a major impact on the regulation of CD19 splicing as RBPs are usually integrated in a defined network with additional translation-effective proteins. Thus, the availability and activity of single splicing factors and regulatory molecules might diversely influence their well-orchestrated synergy with each other (22, 32, 33). Different RBPs including PTBP1 and ZFP36 are embedded in so-called mRNA regulons that coordinately regulate numerous cellular processes including immune response mechanisms (34–37). YTHDC1, for example, is able to promote exon inclusions by recruitment of SRSF3 (30). Moreover, it was shown that PTBP2 can compensate for PTBP1 in B cells, both regulating SRSF3 activity in cancer cells. In turn, SRSF3 and other RBPs modulate PTB protein expression, illustrating that regulatory feedback mechanisms even increase the complexity of splicing events (27, 38–40). Furthermore, RBPs are generally able to modulate splicing of one another. Along this line, predominant splicing isoforms of HNRNPA1 differ between B-ALL and normal pro-B cells, which is accompanied by differences in mRNA stability (29). Similar mechanisms certainly hold true for other RBPs that play a role in disease progression of B-ALL, and likely also for CD19 splicing.

Hence, there is a high diversity of individual factors and regulatory circuits that together decide on the abundance of dedicated protein isoforms. However, it is conceivable that patient-specific features define the isoform distribution of certain proteins including CD19. The disease-specific mutations that we identified can serve as first evidence, differential expression of RBPs binding to those DNA motifs substantiating this idea. Thus, our RNA-Seq data can serve as a source for potential RBP candidates being involved in leukemia-specific and disease-relevant splicing modulation of CD19.

In conclusion, we show that blast-specific mutations in intron regions with regulatory potential exist at diagnosis and that blasts express a complex network of deregulated RBPs that intervene in CD19 splicing. Our data further demonstrate that the entire course of treatment needs to be considered to follow up on disease-specific features that emerging at dedicated time points and establish a CD19 epitope-negative cell population. Consecutive sampling will be critical to identify predictive markers for the likelihood of the emergence of an epitope-negative cell population upon therapy.

Declarations

Competing Interests

The authors declare no competing financial interests.

This project has been funded by the NMFZ program of the University of Mainz and the Gilead funding program.

Author contributions

NZ, MCL, MS, CP were responsible for conducting and evaluating the experiments and preparing the figures. NZ and MS performed statistical analysis. NZ and CP wrote the manuscript. LR provided technical assistance for sample preparation and flow cytometric analysis. NL assisted in the evaluation of the flow cytometry data. SA performed cell sorting. CP, JK and NZ designed the study. FA, KEM, AW, AR, OB provided the patient population. FA and KEM provided guidance for patients' selection. FA and JF obtained the ethical approval for the study. CP and JF were responsible for project administration and supervision. CP, JF and JK acquired the funding. All authors have read and agreed to the published version of the manuscript.

References

1. Maude SL, Frey N, Shaw PA, Aplenc R, Barrett DM, Bunin NJ, et al. Chimeric antigen receptor T cells for sustained remissions in leukemia. N Engl J Med. 2014;371(16):1507-17.
2. Park JH, Riviere I, Gonen M, Wang X, Senechal B, Curran KJ, et al. Long-Term Follow-up of CD19 CAR Therapy in Acute Lymphoblastic Leukemia. N Engl J Med. 2018;378(5):449-59.
3. Sterner RC, Sterner RM. CAR-T cell therapy: current limitations and potential strategies. Blood Cancer J. 2021/04/08 ed2021. p. 69.
4. Shah NN, Fry TJ. Mechanisms of resistance to CAR T cell therapy. Nat Rev Clin Oncol2019. p. 372-85.
5. Maude SL, Laetsch TW, Buechner J, Rives S, Boyer M, Bittencourt H, et al. Tisagenlecleucel in Children and Young Adults with B-Cell Lymphoblastic Leukemia. N Engl J Med. 2018;378(5):439-48.
6. Xu X, Sun Q, Liang X, Chen Z, Zhang X, Zhou X, et al. Mechanisms of Relapse After CD19 CAR T-Cell Therapy for Acute Lymphoblastic Leukemia and Its Prevention and Treatment Strategies. Front Immunol2019. p. 2664.
7. Guo Z, Tu S, Yu S, Wu L, Pan W, Chang N, et al. Preclinical and clinical advances in dual-target chimeric antigen receptor therapy for hematological malignancies. Cancer Sci. 2021/01/09 ed2021. p. 1357-68.
8. Orlando EJ, Han X, Tribouley C, Wood PA, Leary RJ, Riester M, et al. Genetic mechanisms of target antigen loss in CAR19 therapy of acute lymphoblastic leukemia. Nat Med. 2018;24(10):1504-6.

9. Sotillo E, Barrett DM, Black KL, Bagashev A, Oldridge D, Wu G, et al. Convergence of Acquired Mutations and Alternative Splicing of CD19 Enables Resistance to CART-19 Immunotherapy. Cancer Discov. 2015;5(12):1282-95.
10. Asnani M, Hayer KE, Naqvi AS, Zheng S, Yang SY, Oldridge D, et al. Retention of CD19 intron 2 contributes to CART-19 resistance in leukemias with subclonal frameshift mutations in CD19. Leukemia. 2020;34(4):1202-7.
11. Bagashev A, Sotillo E, Tang CH, Black KL, Perazzelli J, Seeholzer SH, et al. CD19 Alterations Emerging after CD19-Directed Immunotherapy Cause Retention of the Misfolded Protein in the Endoplasmic Reticulum. Mol Cell Biol. 2018;38(21).
12. Rabilloud T, Potier D, Pankaew S, Nozais M, Loosveld M, Payet-Bornet D. Single-cell profiling identifies pre-existing CD19-negative subclones in a B-ALL patient with CD19-negative relapse after CAR-T therapy. Nat Commun. 2021;12(1):865.
13. Fischer J, Paret C, El Malki K, Alt F, Wingerter A, Neu MA, et al. CD19 Isoforms Enabling Resistance to CART-19 Immunotherapy Are Expressed in B-ALL Patients at Initial Diagnosis. J Immunother. 2017;40(5):187-95.
14. Giudice G, Sanchez-Cabo F, Torroja C, Lara-Pezzi E. ATtRACT-a database of RNA-binding proteins and associated motifs. Database (Oxford). 2016;2016.
15. Perez I, Lin CH, McAfee JG, Patton JG. Mutation of PTB binding sites causes misregulation of alternative 3' splice site selection in vivo. RNA. 1997;3(7):764-78.
16. Feng H, Bao S, Rahman MA, Weyn-Vanhentenryck SM, Khan A, Wong J, et al. Modeling RNA-Binding Protein Specificity In Vivo by Precisely Registering Protein-RNA Crosslink Sites. Mol Cell. 2019;74(6):1189-204 e6.
17. Spellman R, Llorian M, Smith CW. Crossregulation and functional redundancy between the splicing regulator PTB and its paralogs nPTB and ROD1. Mol Cell. 2007;27(3):420-34.
18. Jung H, Lee D, Lee J, Park D, Kim YJ, Park WY, et al. Intron retention is a widespread mechanism of tumor-suppressor inactivation. Nat Genet. 2015;47(11):1242-8.
19. Supek F, Minana B, Valcarcel J, Gabaldon T, Lehner B. Synonymous mutations frequently act as driver mutations in human cancers. Cell. 2014;156(6):1324-35.
20. Darman RB, Seiler M, Agrawal AA, Lim KH, Peng S, Aird D, et al. Cancer-Associated SF3B1 Hotspot Mutations Induce Cryptic 3' Splice Site Selection through Use of a Different Branch Point. Cell Rep. 2015;13(5):1033-45.
21. Quesada V, Conde L, Villamor N, Ordonez GR, Jares P, Bassaganyas L, et al. Exome sequencing identifies recurrent mutations of the splicing factor SF3B1 gene in chronic lymphocytic leukemia. Nat Genet. 2011;44(1):47-52.
22. Climente-Gonzalez H, Porta-Pardo E, Godzik A, Eyras E. The Functional Impact of Alternative Splicing in Cancer. Cell Rep. 2017;20(9):2215-26.
23. Peng Q, Zhou Y, Oyang L, Wu N, Tang Y, Su M, et al. Impacts and mechanisms of alternative mRNA splicing in cancer metabolism, immune response, and therapeutics. Mol Ther. 2021/11/19 ed2021.

24. Galloway A, Saveliev A, Lukasiak S, Hodson DJ, Bolland D, Balmanno K, et al. RNA-binding proteins ZFP36L1 and ZFP36L2 promote cell quiescence. Science. 2016;352(6284):453-9.
25. Zekavati A, Nasir A, Alcaraz A, Aldrovandi M, Marsh P, Norton JD, et al. Post-transcriptional regulation of BCL2 mRNA by the RNA-binding protein ZFP36L1 in malignant B cells. PLoS One. 2014;9(7):e102625.
26. Newman R, Ahlfors H, Saveliev A, Galloway A, Hodson DJ, Williams R, et al. Maintenance of the marginal-zone B cell compartment specifically requires the RNA-binding protein ZFP36L1. Nat Immunol. 2017;18(6):683-93.
27. Monzon-Casanova E, Matheson LS, Tabbada K, Zarnack K, Smith CW, Turner M. Polypyrimidine tract-binding proteins are essential for B cell development. Elife. 2020;9.
28. Monzon-Casanova E, Screen M, Diaz-Munoz MD, Coulson RMR, Bell SE, Lamers G, et al. The RNA-binding protein PTBP1 is necessary for B cell selection in germinal centers. Nat Immunol. 2018;19(3):267-78.
29. Black KL, Naqvi AS, Asnani M, Hayer KE, Yang SY, Gillespie E, et al. Aberrant splicing in B-cell acute lymphoblastic leukemia. Nucleic Acids Res. 2018;46(21):11357-69.
30. Xiao W, Adhikari S, Dahal U, Chen YS, Hao YJ, Sun BF, et al. Nuclear m(6)A Reader YTHDC1 Regulates mRNA Splicing. Mol Cell. 2016;61(4):507-19.
31. Katsuyama T, Moulton VR. Splicing factor SRSF1 is indispensable for regulatory T cell homeostasis and function. Cell Rep. 2021;36(1):109339.
32. Van Nostrand EL, Freese P, Pratt GA, Wang X, Wei X, Xiao R, et al. A large-scale binding and functional map of human RNA-binding proteins. Nature. 2020;583(7818):711-9.
33. Sciarrillo R, Wojtuszkiewicz A, Assaraf YG, Jansen G, Kaspers GJL, Giovannetti E, et al. The role of alternative splicing in cancer: From oncogenesis to drug resistance. Drug Resist Updat. 2020/10/19 ed2020. p. 100728.
34. Diaz-Munoz MD, Osma-Garcia IC. The RNA regulatory programs that govern lymphocyte development and function. Wiley Interdiscip Rev RNA. 2021:e1683.
35. Diaz-Munoz MD, Turner M. Uncovering the Role of RNA-Binding Proteins in Gene Expression in the Immune System. Front Immunol. 2018;9:1094.
36. Turner M, Diaz-Munoz MD. RNA-binding proteins control gene expression and cell fate in the immune system. Nat Immunol. 2018/01/20 ed2018. p. 120-9.
37. Keene JD. RNA regulons: coordination of post-transcriptional events. Nat Rev Genet. 2007;8(7):533-43.
38. Guo J, Jia J, Jia R. PTBP1 and PTBP2 impaired autoregulation of SRSF3 in cancer cells. Sci Rep. 2015;5:14548.
39. Zhou Z, Gong Q, Lin Z, Wang Y, Li M, Wang L, et al. Emerging Roles of SRSF3 as a Therapeutic Target for Cancer. Front Oncol. 2020;10:577636.

40. Izquierdo JM, Majos N, Bonnal S, Martinez C, Castelo R, Guigo R, et al. Regulation of Fas alternative splicing by antagonistic effects of TIA-1 and PTB on exon definition. Mol Cell. 2005;19(4):475-84.

Figures

Figure 1

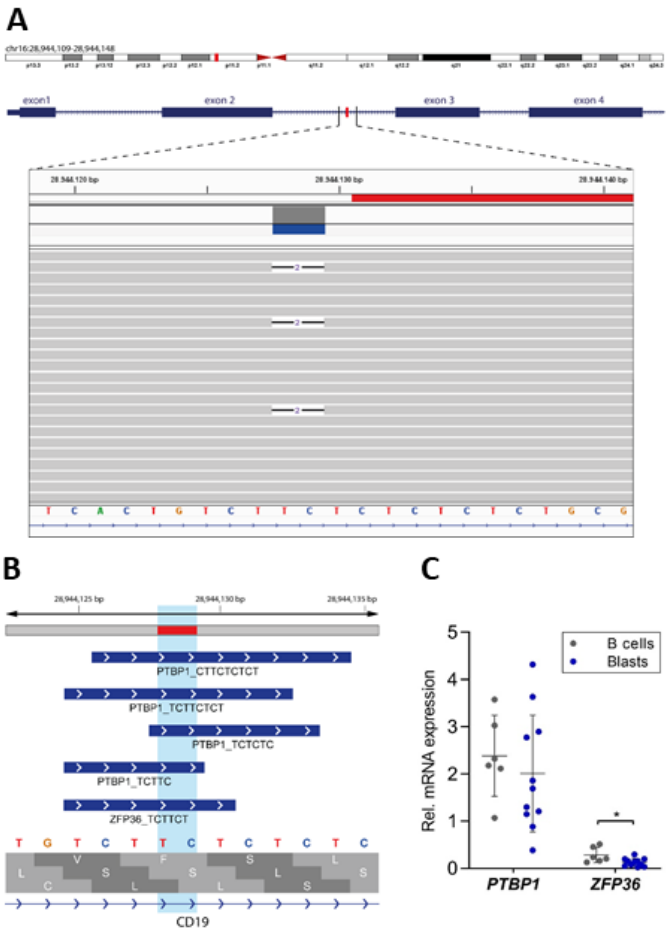

Figure 1

A blast-specific mutation in CD19 intron 2 affects RBP binding domains

(A) Localization of CD19 on chr.16 p11.2 (upper panel, red square) and overview of CD19 exon 1-4. The position of the mutation in intron 2 is indicated in red. Detailed view of the DNA segment harboring the mutation site and single reads carrying the TTC>T mutation (lower panel). Alignments are visualized with Integrative Genomics Viewer (IGV). (B) RBPs and binding motifs overlapping the mutated DNA locus. Nucleotides being affected by the deletion are highlighted in light blue. All binding motifs ≥5 nucleotides suggested by ATtRACT are displayed. (C) qRT-PCR analysis of *PTBP1* and *ZFP36* in sorted B cells and leukemic blasts of pediatric healthy donors and B-ALL patients (n=6 patients in control, n=11 patients in diseased group; *, $p<0.05$).

Figure 2

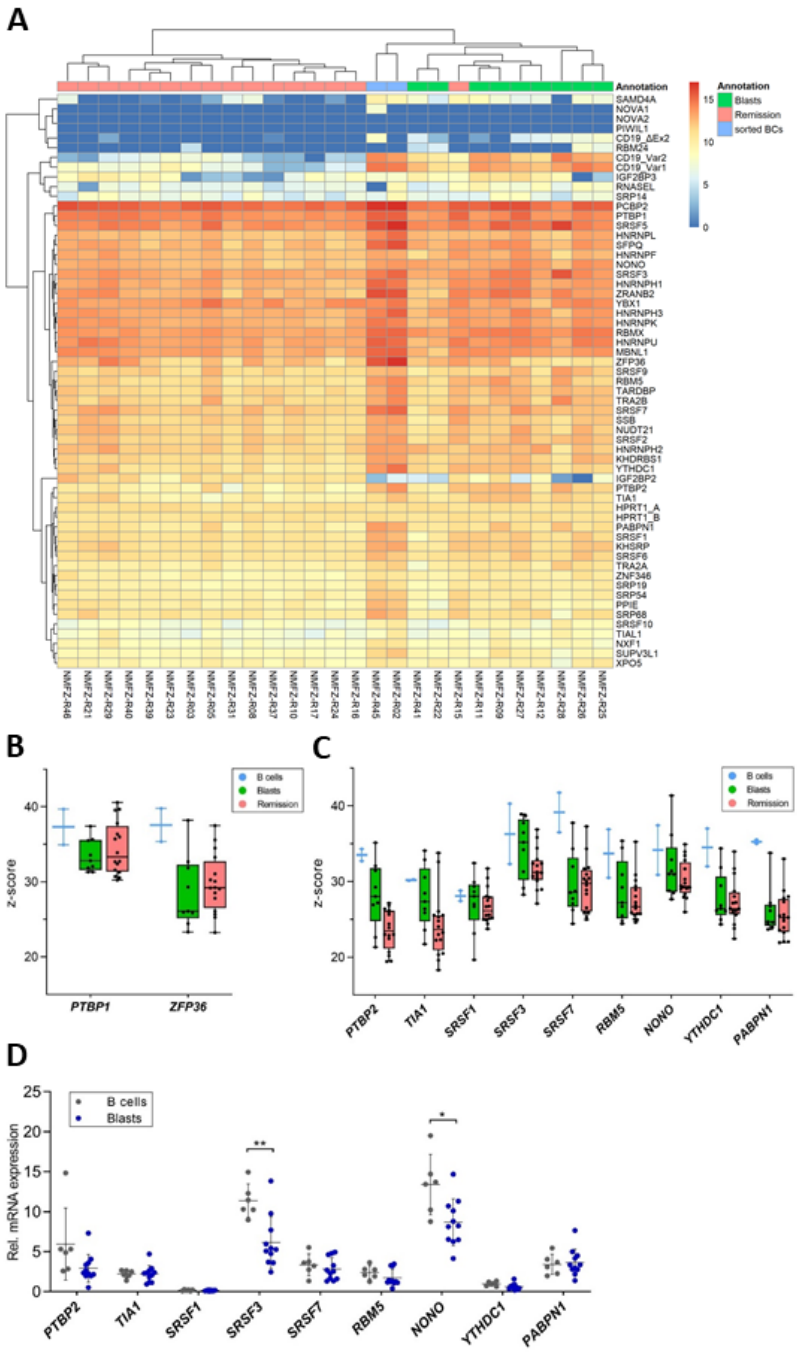

Figure 2

B-ALL patients exhibit disease-specific RBP expression profile

(A) Heatmap visualization of RNA-Seq data from patients at diagnosis, in remission and sorted B-cells from healthy donors. RBP expression is shown as log-transformed data normalized to *HPRT*. (B, C) Boxplots of z-standardized, log-normalized RNA-Seq counts of RBPs. Error bars indicate min to max

values. (D) qRT-PCR analysis of selected RBPs in sorted B cells and leukemic blasts of pediatric healthy donors and B-ALL patients (n=6 patients in control, n=11 patients in diseased group; *, p<0.05; **, p<0.01).

Figure 3

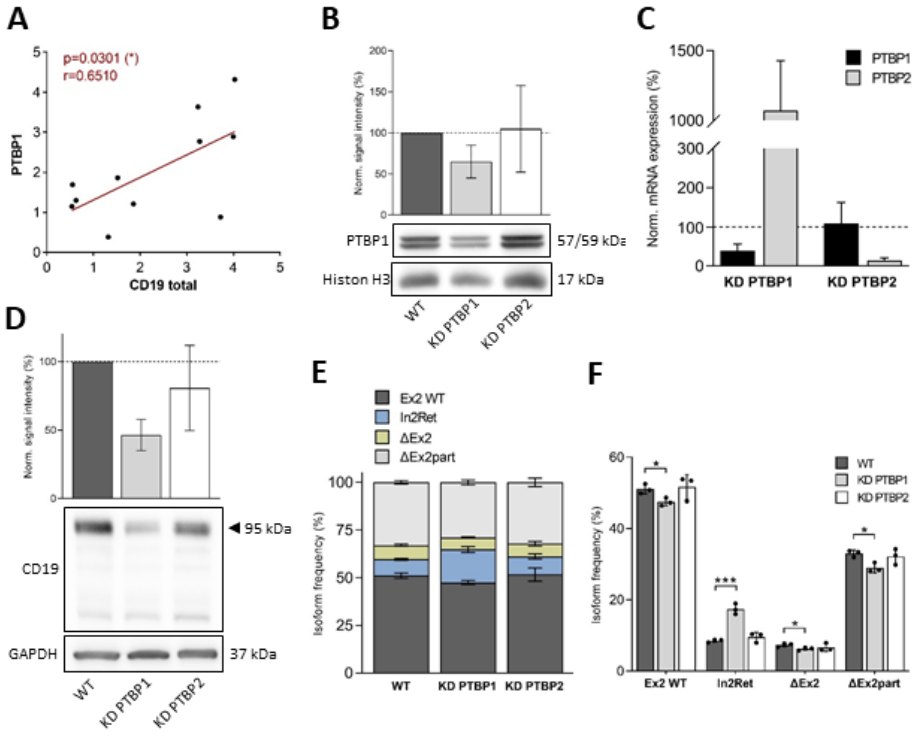

Figure 3

PTBP1 regulates CD19 protein expression by modulating alternative splicing of intron 2

(A) Correlation analysis of *CD19* and *PTBP1* mRNA expression levels in sorted blasts of patients at initial diagnosis (n=11). Simple linear regression and fit line was calculated using GraphPad Prism software. (B) Western blots for PTBP1 of 697 cells after nucleofection without (WT) or with target specific gRNAs for PTBP1 and PTBP2. Histon H3 served as loading control. Quantification was normalized to the WT control set to 100% (n=4 independent experiments). (C) Normalized mRNA expression of *PTBP1* and *PTBP2* in control cells (100%) and in *PTBP1* and *PTBP2* KD cells. (D) Western blot for CD19 and quantification shown as signal intensity relative to WT cells (100%) (n=3 independent experiments). (E, F) qRT-PCR analysis of *Ex2WT*, *In2Ret*, *ΔEx2* and *ΔEx2part* in the same cells. Normalized expression values are calculated as percentage of all Ex2-related CD19 isoforms. Data is shown as stacked graph (E) and bar graph for better visualization of statistical differences (F) (n=3 independent experiments; *, $p<0.05$; ***, $p<0.001$).

Figure 4

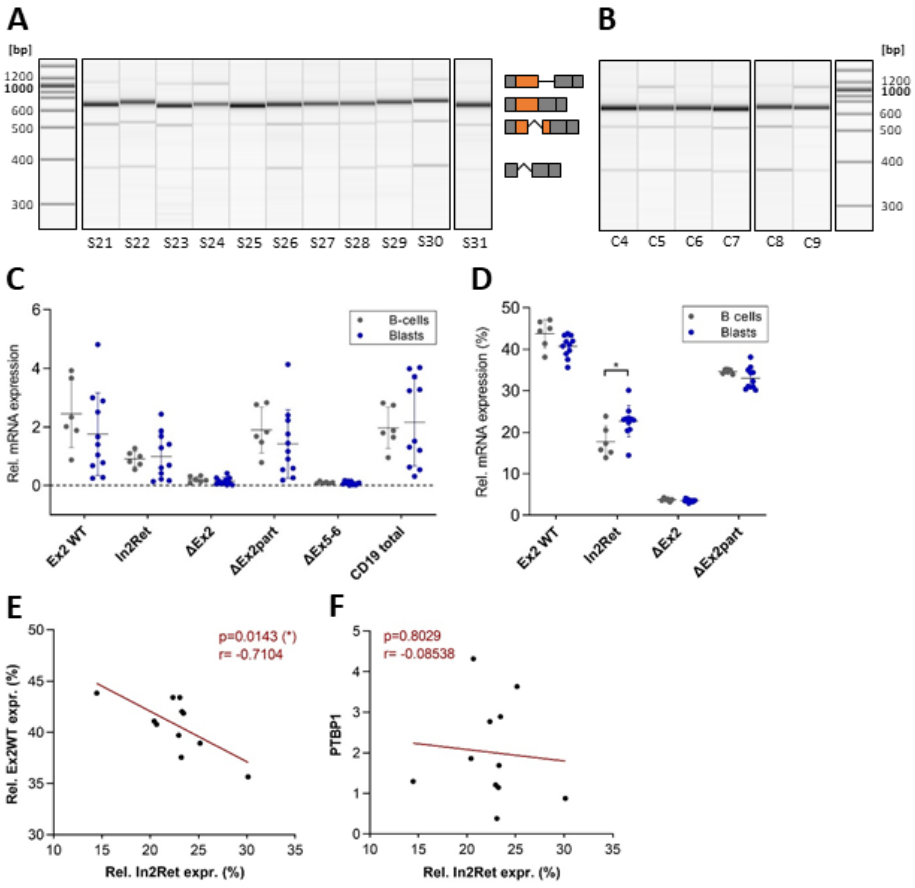

Figure 4

Intron 2 retention is not disease-specific but increased in leukemic blasts

(A, B) Capillary gel electrophoresis of semi-quantitative RT-PCR visualizing CD19 exon 2 isoforms in leukemic blasts (A) and normal B cells (B). Primers spanning exon 1-4 were used. Isoforms from top to bottom: *In2Ret, Ex2 WT, ΔEx2part, ΔEx2*. (C) qRT-PCR analysis of CD19 isoforms in sorted B cells and

leukemic blasts of pediatric healthy donors and B-ALL patients, respectively. (D) Percentage of CD19 exon 2 isoforms. Calculations were performed using the same raw values as in C (n=6 patients in control, n=11 patients in diseased group). (E, F) Analysis correlating the percentage of *In2Ret* and *Ex2 WT* (E) or *PTBP1* (F) expression in leukemic blasts (n=11). Simple linear regression and fit line was calculated using GraphPad Prism software. *, $p<0.05$.

Supplementary Files

This is a list of supplementary files associated with this preprint. Click to download.

- TableS1.docx
- Suppl.Informationcombined.pdf